Implementation of Optical Perfect Shuffle with Substrate Guided-Wave Optical Interconnects

Jian Liu, *Student Member, IEEE,* Chunhe Zhao, and Ray T. Chen, *Member, IEEE*

***Abstract*— The vulnerability in optoelectronic packaging of free space optical interconnects fail to provide a reliable interconnection for highly parallel system. In this letter, we report, for the first time, a substrate-guided-wave-based perfect shuffle (PS) having an 8-to-8 interconnection, is demonstrated at 632.8-nm wavelength. Sixteen waveguide holograms are fabricated with the full functionality of the PS. The diffraction efficiencies of the waveguide holograms are all within 80% ±5%. The surface-normal configuration of the demonstrated PS makes the integration with vertical-cavity surface-emitting lasers (VCSEL's) and other surface-mountable processing elements (PE's) highly feasible.**

***Index Terms*— Optical interconnects, optical perfect shuffle, parallel processing, photopolymer films, volume hologram.**

I. Introduction

IN PARALLEL computing architecture, the perfect shuffle (PS) is proven to be an efficient interconnection method for parallel processing algorithms, such as the fast Fourier transform (FFT), polynomial evaluation, sorting, and matrix transposition [1]. For high-speed (>1 GHz) parallel processing, the performance of the existing communication links among processing elements (PE's) based on microelectronic integrated circuits is limited by electromagnetic interference, parasitic capacitance, and inductance coupling. To overcome the bottlenecks of electrical interconnects, optical interconnection has been widely agreed to be one of the most important alternatives [2], [3].

Many investigators have been working on optical implementation of the perfect shuffle, and several approaches have been proposed and then demonstrated [4]–[9]. Lohmann and his colleague [4], [5] performed this concept with a combination of lenses and prisms. Using microlens arrays, the PS is demonstrated by Sawchuk and Glaser [6]. Recently, holographic optical elements (HOE's) are employed to implement one-dimensional (1-D) and two-dimensional (2-D) PS's [7]–[9]. All these implementations are limited to free space optical interconnects, which are vulnerable to mechanical and environmental perturbations. Furthermore, extra components like lenses and/or prisms are always needed to route optical signals.

Manuscript received February 11, 1997; revised April 10, 1997. This work was supported by the Air Force Office of Scientific Research, Ballistic Missile Defense Organization, Office of Naval Research, Cray Research, DuPont, and the ATP program of the State of Texas.

The authors are with the Department of Electrical and Computer Engineering, Microelectronics Research Center, University of Texas at Austin, Austin, TX 78758 USA.

Publisher Item Identifier S 1041-1135(97)05021-0.

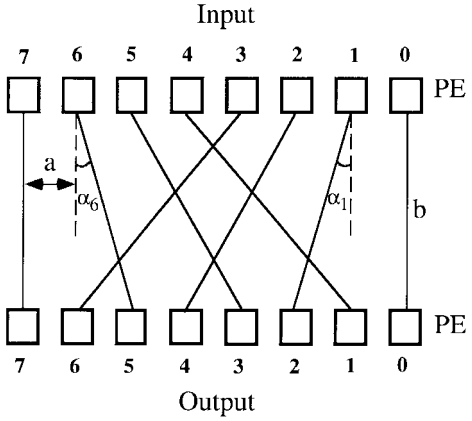

Fig. 1. Schematic diagram for the perfect shuffle (PS) interconnection with $N = 8$ PE's. The small boxes represent PE's.

Substrate guided wave optical interconnects, using HOE's combined with total internal reflection (TIR) in dielectric or semiconductor substrates, have been demonstrated as efficient approaches for intra- and inter-module interconnections, optical clock distributions, and optical backplane buses [10]. In this letter, we present, for the first time, the PS implemented by using HOE based substrate guided wave optical interconnects.

For a computing cluster having $N = 2^k$ PE's, the PS-bared optical interconnection divides this group into two subgroups and then interlaces the PE's from the first subgroup to the second subgroup with a one-to-one interconnection. The PS is generally defined mathematically as [1]

$$n' = \begin{cases} 2n, & \text{for } 0 \le n \le \dfrac{N}{2} - 1 \\ 2n - N + 1, & \text{for } \dfrac{N}{2} \le n \le N - 1 \end{cases} \tag{1}$$

where n' is the new location of the nth PE. An interconnection of a PS having 8 PE's is shown in Fig. 1. The first PE subgroup located at 0, 1, 2, 3 will be shuffled to new positions numbered by 0, 2, 4, 6, respectively. The other subgroup with locations 4, 5, 6, 7 will be interlaced to positions 1, 3, 5, 7, respectively. Assume the distance between the two adjacent PE's in both input and output nodes is a and the distance separating the input and output nodes is b, as shown in Fig. 1, the angle α_n steering an input signal to its designated output nodes is

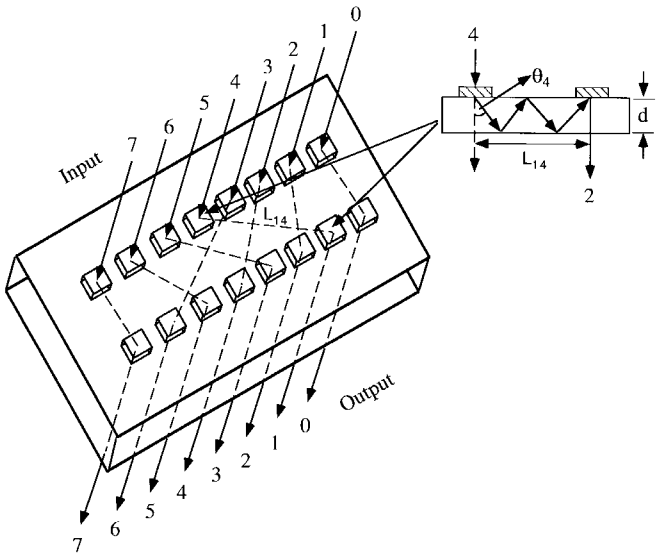

Fig. 2. Integration of eight pairs of HOE's on one waveguiding plate. Interconnection in the waveguiding plate between the fourth PE of the input group and first PE of the output group is shown in the inset as an example.

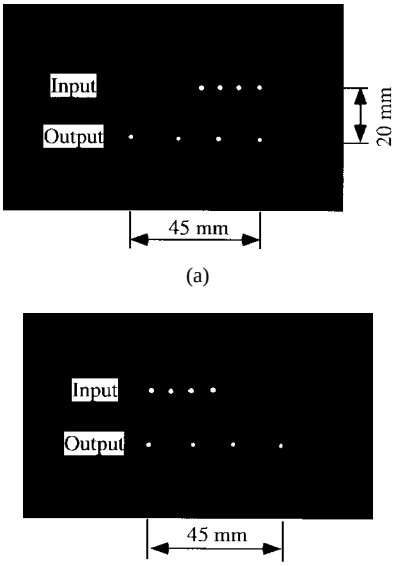

Fig. 3. Experimental results of the PS interconnection with eight PE's: (a) interconnecting result for the first subgroup ($0 \rightarrow 0$, $1 \rightarrow 2$, $2 \rightarrow 4$, $3 \rightarrow 6$) and (b) interconnecting result for the second subgroup ($4 \rightarrow 1$, $5 \rightarrow 3$, $6 \rightarrow 5$, $7 \rightarrow 7$).

given by

$$\alpha_n = \begin{cases} \tan^{-1}\left(\dfrac{na}{b}\right) & \text{for } 0 \le n \le \dfrac{N}{2} - 1 \\ \tan^{-1}\left[\dfrac{(n-N+1)a}{b}\right] & \text{for } \dfrac{N}{2} \le n \le N-1. \end{cases} \tag{2}$$

Equation (2) is used in our experiment for fabricating the corresponding HOE's.

DuPont photopolymers HRF 600X001-20 (20 μm thick) are selected as the holographic films due to their dry processing, long shelf life, good photospeed, and large index modulation properties [11]–[14]. This type of material is advantageous when considering the wet-processing requirement affiliated with DCG [15]. The volume holographic grating formation mechanism in the photopolymer is known to be a three-step process [11]. First, an initial exposure records the interference pattern, which causes initial polymerization and diffusion of the monomer molecules to the bright fringe area from the dark fringe neighborhood within the photopolymer. A higher concentration of polymerization means a higher refractive index. Second, a uniform UV light is required for dye bleaching and complete polymerization of the photo-sensitive polymer. Third, a baking process further enhances the index modulation of the hologram formed.

To experimentally carry out the PS with eight pairs of PE's shown in Fig. 1 using HOE-based substrate guided wave optical interconnects, eight input HOE's are integrated on a glass substrate to direct the input signals to the desired directions. The signals are eventually coupled out of the substrate by another corresponding output HOE's as shown in Fig. 2. A two-beam interference method [10] is employed to fabricate both the input and output HOE's. An Argon ion laser operating at 514 nm is used in the hologram recording. For demonstration purpose, the reconstruction wavelength is set at 632.8 nm. The diffraction angle for each HOE, which is greater than the critical angle of a BK7 glass waveguiding plate, is designed to be

$$\theta_n = \tan^{-1}\left(\frac{L_{n'n}}{2md}\right) \tag{3}$$

where $L_{n'n}$ is the distance interconnecting n'th and nth HOE's, d is the thickness of the substrate glass, and m is an integer representing the maximum number of the zigzag bouncing with a distance of $2d$ in the substrate between the n'th and the nth HOE's. The Bragg condition [16] and the Snell's law are applied to calculate the diffraction angle in the holographic medium and then to convert the recording angles to those in the air. For each interconnection, two individual photopolymer films are laminated on the waveguiding plate ($\sim$3.35-mm thick) at the designated positions and volume holograms are then recorded in the films. An optical signal coupled in by an input HOE is totally internal-reflected and then correctly guided within the waveguiding plate at a diffraction angle defined by (3). The zigzagged signal beam is finally coupled out by the output HOE. Eight pairs of HOE's are sequentially fabricated on the same waveguiding plate at the desired locations as indicated in Fig. 2. The integration of the HOE's on a solid waveguiding substrate makes the PS robust to mechanical and environmental perturbations when compared with free-space interconnects and which, with a surface normal configuration, makes the optoelectronic packaging much more reliable in conjunction with the surface-mount technology (SMT). In our experiment, the angles of rotation for eight pairs of HOE's are designed to be 0° (0 $\rightarrow$ 0), 20.5° (1 $\rightarrow$ 2), 37° (2 $\rightarrow$ 4), 48.3° (3 $\rightarrow$ 6), $-$48.3° (4 $\rightarrow$ 1), $-$37° (5 $\rightarrow$ 3), $-$20.5° (6$\rightarrow$ 5), and 0° (7 $\rightarrow$ 7), the two numbers within the parentheses are the corresponding input and output nodes, respectively; and the corresponding bouncing angles are 45° ($n = 0$), 46.3° ($n = 1$), 43° ($n =$

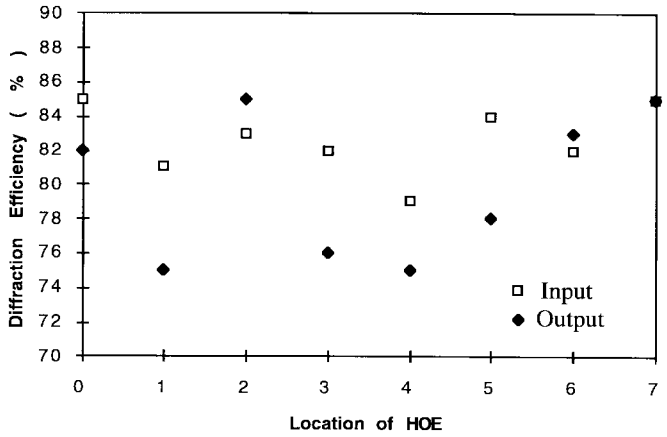

Fig. 4. Measured diffraction efficiencies for the eight pairs of HOE's.

TABLE I
INTERCONNECTION ALLOCATIONS AMONG INPUT AND OUTPUT NODES

n	0	1	2	3	4	5	6	7
n'	0	2	4	6	1	3	5	7

2), 43.2° ($n = 3$), 43.2° ($n = 4$), 43° ($n = 5$), 46.3° ($n = 6$), and 45° ($n = 7$).

Eight input beams with s-polarization are used as the input optical signals for the PS device. Table I gives the interconnection nodes between input and output optical signals. Fig. 3(a) shows the transform of the first subgroup ($0 \rightarrow 0$, $1 \rightarrow 2$, $2 \rightarrow 4$, $3 \rightarrow 6$). Other permutations corresponding to the second subgroup ($4 \rightarrow 1$, $5 \rightarrow 3$, $6 \rightarrow 5$, $7 \rightarrow 7$) are shown in Fig. 3(b). In Fig. 3, the input optical signals are also included in the photos to clearly show the PS operation. The diffraction efficiencies of all HOE's are measured and the results are shown in Fig. 4. All data are within 80% $\pm$5%. The surface-normal input signals are diffracted by the input HOE's and are successfully coupled out in the surface-normal direction at the desired locations. Among all the interconnect scenarios, there is no crosstalk observed. Such a configuration is pivotal for implementing surface normal transceivers such as vertical cavity surface emitting lasers (VCSEL's) [17], [18] and resonant cavity photodetector [19]. One disadvantage of the device is the optical signal experiences twice the loss of the input and output HOE diffraction efficiencies.

Other than the PS interconnection for parallel processing algorithms, this method can also be used to implement other communication networks critical to parallel computing. These include butterfly and crossover interconnections, and multistage networks [20], [21].

II. CONCLUSION

A novel approach to implement the optical PS interconnection by the photopolymer HOE based substrate guided wave optical interconnects is proposed. Preliminary experimental results operating at 632.8 nm proves the feasibility. Several advantages are demonstrated using this method. First, the perfect shuffle interconnection can be easily achieved by the surface-normal input and output HOE's integrated on the waveguiding plate. The photopolymer films employed can be easily laminated on the substrate. Second, the integration of the HOE's on a solid waveguiding substrate makes the PS robust against mechanical and environmental perturbations when compared with free-space interconnects and which makes the optoelectronic packaging much more reliable. Finally, the surface-normal configuration makes easy the integration with VCSEL arrays, and other surface-mountable PE's.

ACKNOWLEDGMENT

The authors acknowledge helpful discussion with Dr. De-Gui Sun.

REFERENCES

[1] H. S. Stone, "Parallel processing with the perfect shuffle," *IEEE Trans. Comput.*, vol. C-20, pp. 153–161, 1971.
[2] J. W. Goodman, F. I. Leonberger, S. Y. Kung, and R. A. Athale, "Optical interconnection for VLSI systems," *Proc. IEEE*, vol. 72, pp. 850–866, 1984.
[3] T. Yatagai, S. Kawai, and H. Huang, "Optical computing and interconnects," *Proc. IEEE*, vol. 84, pp. 828–852, 1996.
[4] A. W. Lohmann, "What classical optics can do for the digital optical computer," *Appl. Opt.*, vol. 25, pp. 1543–1549, 1986.
[5] A. W. Lohmann, W. Stork, and G. Stucke, "Optical perfect shuffle," *Appl. Opt.*, vol. 25, pp. 1530–1531, 1986.
[6] A. A. Sauchuk and I. Glaser, "Geometries for optical implementations of the perfect shuffle," in *Proc. SPIE*, 1989, vol. 963, pp. 270–282.
[7] H. Kang, Y. Zhan, J. Zhang, X. Huang, and X. Zhu, "Optical perfect-shuffle network implementation by use of an ordinary imaging system and holographic gratings," *Appl. Opt.*, vol. 33, pp. 2988–2990, 1994.
[8] N. Davidson, A. A. Friesem, and E. Hasman, "Realization of perfect shuffle and inverse perfect shuffle transforms with holographic elements," *Appl. Opt.*, vol. 31, pp. 1810–1812, 1992.
[9] J. M. Wang, L. Cheng, and A. A. Sawchuk, "Light-efficient two-dimensional perfect shuffles with DuPont photopolymer holograms," *Appl. Opt.*, vol. 32, pp. 7148–7154, 1993.
[10] R. T. Chen, C. Zhou, C. Zhao, and R. Lee, "Photopolymer-based waveguide holograms for optoelectronic interconnects applications," *Critical Rev. Optical Sci. Technol.*, vol. CR-63, pp. 46–64, 1996.
[11] W. Gambogi, K. Steijn, S. Mackara, T. Duzik, B. Hamzavy, and J. Kelly, "HOE imaging in DuPont holographic photopolymers," in *Proc. SPIE*, 1994, vol. 2152, pp. 282–293.
[12] U. Rhee, H. J. Caulfield, C. S. Vikram, and J. Shamir, "Dynamics of hologram recording in DuPont photopolymer," *Appl. Opt.*, vol. 34, pp. 846–853, 1995.
[13] S. Piazzolla and B. K. Jenkins, "Holographic grating formation in photopolymers," *Opt. Lett.*, vol. 21, pp. 1075–1077, 1996.
[14] H. J. Zhou, V. Morozov, and J. Neff, "Characterization of DuPont photopolymers in infrared light for free-space optical interconnects," *Appl. Opt.*, vol. 34, pp. 7457–7459, 1995.
[15] T. G. Georgekutty and H. K. Liu, "Simplified dichromated gelatin hologram recording process," *Appl. Opt.*, vol. 26, pp. 372–376, 1987.
[16] H. Kogelnik, "Coupled wave theory for thick hologram gratings," *The Bell Syst. Tech. J.*, vol. 13, pp. 2909–2947, 1969.
[17] D. L. Huffaker, L. A. Graham, and D. G. Deppe, "Fabrication of high-packing-density vertical cavity surface emitting laser arrays using selective oxidation," *IEEE Photon. Technol. Lett.*, vol. 8, pp. 596–598, 1996.
[18] D. G. Deppe, D. L. Huffaker, J. Shin, and Q. Deng, "Very-low-threshold index-confined planar microcavity lasers," *IEEE Photon. Technol. Lett.*, vol. 7, pp. 965–967, 1995.
[19] H. Nie, K. A. Anselm, C. Hu, S. S. Murtaza, B. G. Streetman, and J. C. Campbell, "High-speed resonant-cavity separate absorption and multiplication avalanche photodiodes with 130 GHz gain-bandwidth product," *Appl. Phys. Lett.*, vol. 70, pp. 161–163, 1997.
[20] C. Tocci and H. J. Caulfield, *Optical Interconnection.* Boston, MA: Artech House, 1994.
[21] D. G. Sun, N. Wang, L. He, M. Xu, G. Liang, and J. Zheng, "Research on optical multistage butterfly interconnection and optoelectronic logic operations," *Opt. Laser Technol.*, vol. 26, pp. 379–383, 1994.